Characterization of Scintillation Tile Beam Intensity Monitor for the Trigger of XBPF

Shota Kondo
Supervisor: Emma Buchanan and Inaki Ortega

September 1st 2023

Abstract

New beam intensity monitor and trigger generator is needed in the CERN North Experimental Area because of the problems of current one such as aging and incompatibility to the new beam profile monitor. In this study, I characterized the response of new beam intensity monitor and trigger generator composed of scintillation tile and wavelength shifting fiber. The result shows that the response depends on the radiation injected position and the photon detection efficiency exceeds the goal of 99% when the threshold is set as 3 photons for each SiPM put on left and right of the detector. As well as this, the result shows that wrapping detector by reflective foil such as aluminum foil can improve the photon detection capability of the detector.

1 Introduction

In this study, I characterized the response of scintillation tile detector which will be used as beam intensity monitor and trigger generator in CERN North Experimental Area. Currently, scintillation paddle is used as one of the beam intensity monitor and trigger generator. However, it has been used tens of years and the effect of aging appears. In addition, it is not compatible to the new beam profile monitor XBPF because of its large dimension and less mobility. XBPF is put in the vacuum tank in the beam line and motored to insert to and extract from the beam path. Thus, scintillation tile detector which can be made compact is more compatible than scintillation paddle and has capability to replace it.

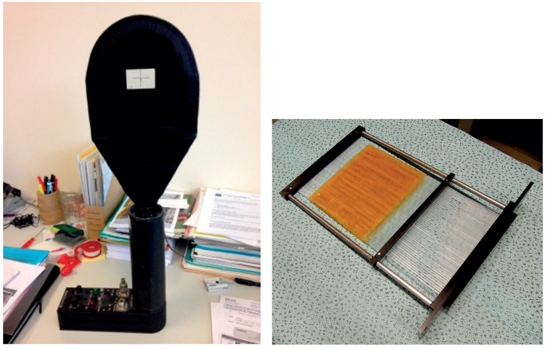

Scintillation paddle XBPF

Figure 1: Scintillation paddle currently used as beam intensity monitor and trigger generator (left). The detector is composed of hemisphere shape plastic scintillator, light guide, and photo multiplier tube. XBPF, new beam profile monitor used in CERN Experimental Area (right). It is inserted to beam path before beam profile monitoring starts and extracted from there after monitoring. [1]

2 Composition and Assembly of Scintillation Tile Detector

Scintillation tile detector is composed of one scintillation tile and two wavelength shifting fiber. If particle beam passes through the tile, it emits UV light. Then, it is absorbed and converted to visible light by fiber. Finally, the light is detected by SiPM put on one end of the fiber. The tile has area of 10×10 cm^2 and thickness of 1.1 mm. Fiber has diameter of 1 mm and is cut to 30 cm length. After cutting, I polished the end of fiber by using three different sandpapers which has different finesse to improve the optical coupling of fiber and SiPM. Then, I connected the tile and fiber by the optical glue (norland optical adhesive 61). Each fiber is put on the opposite edge of the tile, which enables to cutoff the noise by making coincidence of signals from two fibers.

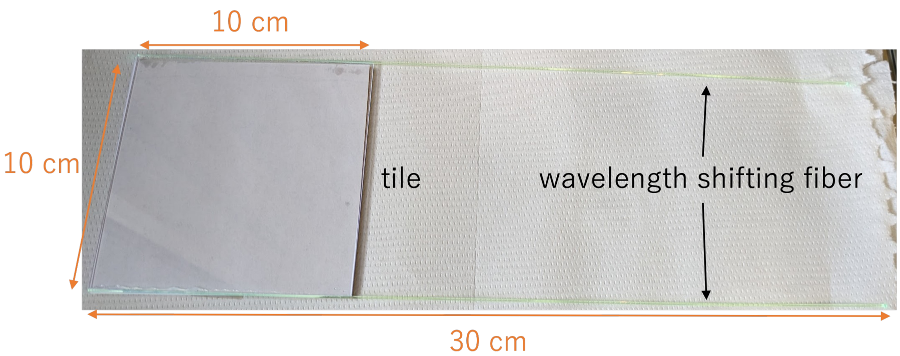

Figure 2: Scintillation tile detector I made.

3 Characterization of SiPM

At first, I characterize the response of SiPM by measuring dark pulse. Sensitive surface of SiPM is divided to huge amount of regions called pixel, and each pixel has capability to detect just one photon. Signal of SiPM is the sum of signal from all pixels, so it is necessary to calibrate the signal corresponds to one photon to quantify the detected number of photon. Dark pulse is the fake signal caused by thermally generated career in the pixel which appears randomly and is rarely generated simultaneously in many pixels. It means most dark pulses correspond to fake one photon signal, so it enables to calibrate the signal of one photon event. In addition, the event rate of dark pulse infer the threshold of photon number for the efficient collection of radiation originated photon.

3.1 Setup and Method of Measurement

Fig3 shows the setup of dark pulse measurement. The tile detector is contained in the test frame and put in the black box to shade environmental light. SiPM is connected to amplifier board which is biased as ±5 V and provided high voltage of 56 V by HV supplier on the board.

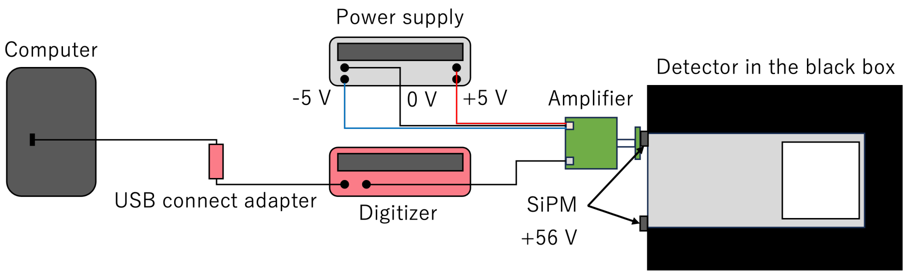

Figure 3: Setup of dark pulse measurement.

Fig4 shows the structure of test frame. It has dent fitting with the size of tile and fiber because the margin fluctuates the position of detector which make the coupling with SiPM bad. SiPM is contained in the beige small container and put on the one edge of fiber. Black tape covered the container to shade the light comes to the space between the frame and the container.

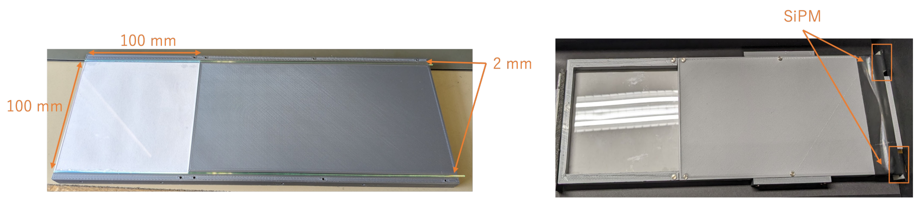

Figure 4: Test frame without cover (left) and with cover (right). The size of dent for the tile is 10×10 cm^2 and that for fiber is 0.2×30 cm^2. Those depth are 0.2 cm.

Measurement was done in this way. First, I measured the signal without threshold then drew the pulse height distribution of obtained events. Fig5 is example of obtained event and Fig6 is the distribution for left and right SiPM. Fig6 shows two obvious peaks, and pulse height of left peak matches that of waveform without threshold in Fig5, so I set the threshold of one photon as 90 which is the border of left peak and right peak. Second, I measured the signal with one photon threshold then determined the threshold of two photons in the same way. I repeated this process until the event rate became small. The number of events is same among all measurement. Also, measurement was done for left and right SiPM alternately because there was only one amplifier board which works correctly.

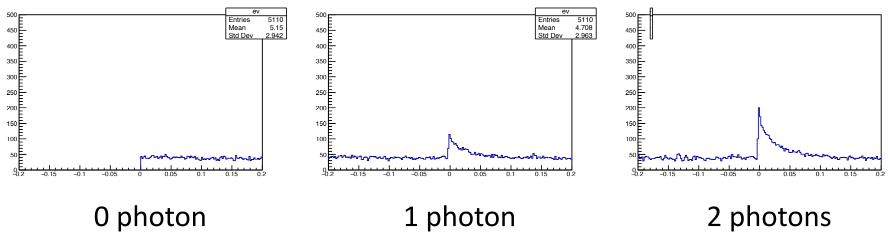

Figure 5: Example of waveform without threshold (left), with one photon threshold (middle), and with two photons threshold (right).

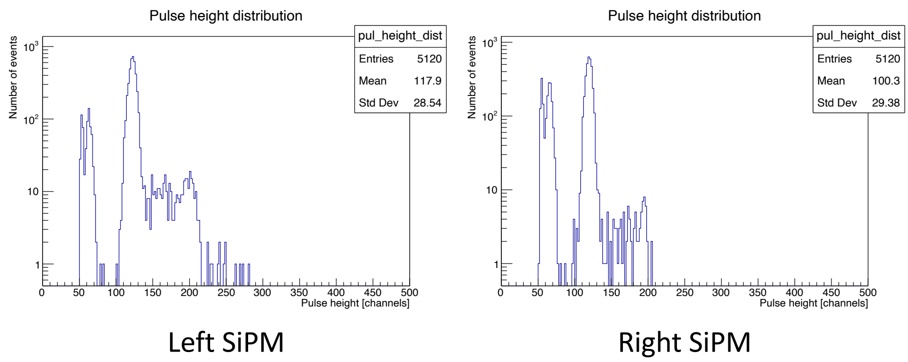

Figure 6: Pulse height distribution without threshold. Left figure is the distribution of left SiPM and right figure is that of right SiPM. There is a border of left and right peak in 90.

3.2 Analysis

I calculated two values from the obtained data. One is integrated pulse which was used to calibrate signals of one photon. To calculate this, firstly, I determined three parameters, pedestal, start bin of pulse in the waveform, and pulse width from mean of Gaussian fit of the distribution with one photon threshold. Table1 shows the obtained parameters. Then, I calculated integrated pulse by the formula below.

$$\text{Integrated pulse} = \sum_{i=\text{Start bin}}^{\text{Start bin+Pulse width}} \text{Pulse height of } i\text{th bin} \tag{1}$$

Another is event rate which was used to determined the threshold for radiation measurement. This value was calculated from number of events and time stamp of digitizer.

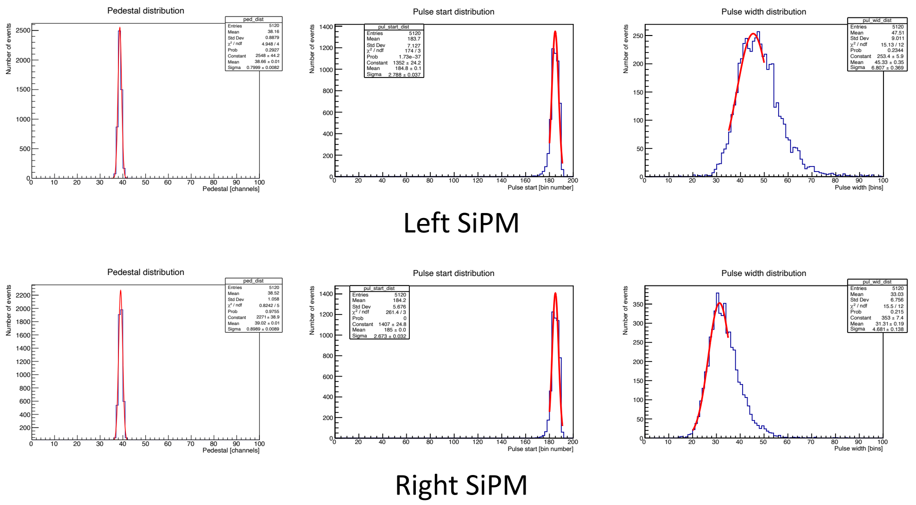

Figure 7: Distribution of pedestal (left), start bin of pulse in the waveform (middle), and pulse width (right). Top figures are from left SiPM and bottom figures are from right SiPM. Red line shows Gaussian fit.

Table 1: Parameters obtained from the distribution with one photon threshold.

	Pedestal	Start bin of pulse	Pulse width
Left SiPM	38.7	185	45
Right SiPM	39.0	185	31

3.3 Result

Fig8 shows the integrated pulse distribution. Red line shows the fitting curve of dark pulse signal (three Gaussian) and background (Landau), and gray line shows the background (Landau) only. From left, peaks correspond to one, two, and three photons which appear with same interval. This interval corresponds to signal of one photon. I obtained the calibration formula converting signal to photon number ($y = p1 \cdot x + p0$) by fitting the plot of mean values of each Gaussian peak.

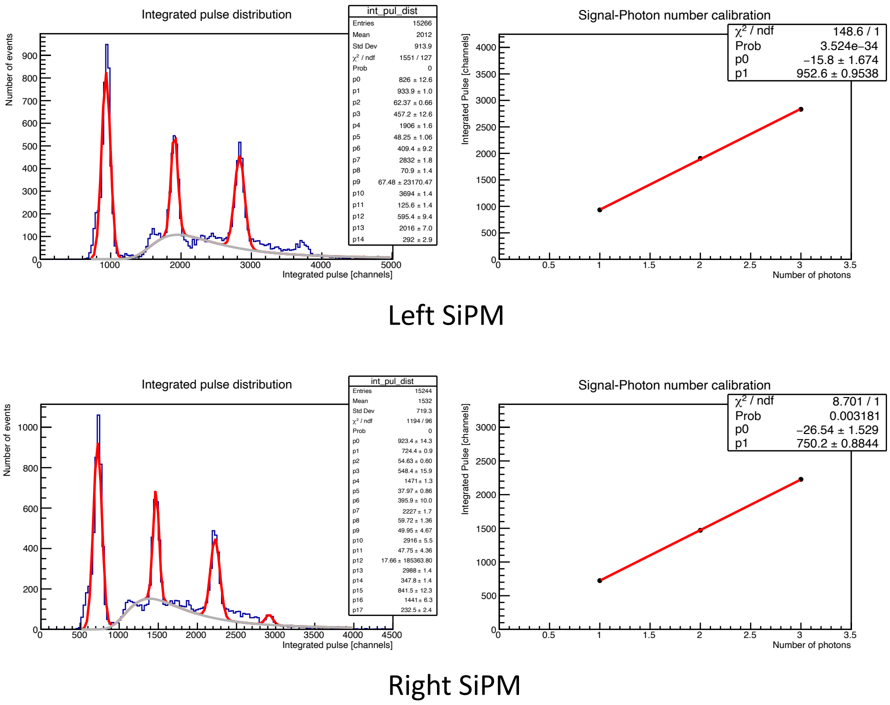

Figure 8: Integrated pulse distribution of dark pulse (left) and calibration formula converting signal to photon number, $y = p1 \cdot x + p0$ (right). Top shows the result of left SiPM and bottom shows that of right SiPM.

Table2 shows the event rate of dark pulse. Event rate of three photons is enough small compared to that of measurement with radiation source (about 1 kHz), so I set the threshold of radiation measurement as three photons.

Table 2: Event rate of dark pulse.

	one photon	two photons	three photons
Left SiPM	1108	1097	84
Right SiPM	1121	1074	18

4 Radiation Source Measurement

To characterize the response of scintillation tile detector, I used three values, mean detected photon number, total detected photon number, and photon detection efficiency obtained from the measurement with radiation source ^{90}Sr. These values were compared among three different types of scintillation tile detector. Also, dependence of detected photon number on the radiation injected point, which is supposed by previous study of Geant4 simulation[2], was validated.

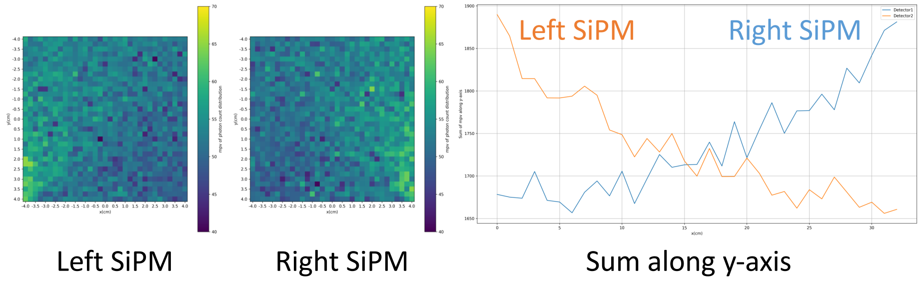

Figure 9: Position dependence of detected photon number obtained by Geant4 simulation. In the left figure which shows the result of left SiPM, wavelength shifting fiber is put along y-axis of $x = 0$, and SiPM is put on one end of the fiber of $y = 0$ side. Similarly, in the middle figure which shows the result of right SiPM, wavelength shifting fiber is put along y-axis of $x = 10$, and SiPM is put on one end of the fiber of $y = 0$ side. Right figure is the sum of mean photon number along y-axis. [2]

4.1 Setup and Method of Measurement

To validate the position dependence, I divided the tile into nine regions and measured its response with radiation source put 4 cm above the center of each region. As I wrote in the end of section 3, I put the threshold as three photons. In addition, measurement was done for three different types of detector, bear one, one with diffusive reflective paint (EJ-510), and one with aluminum foil. Other setup is same as that of dark pulse measurement.

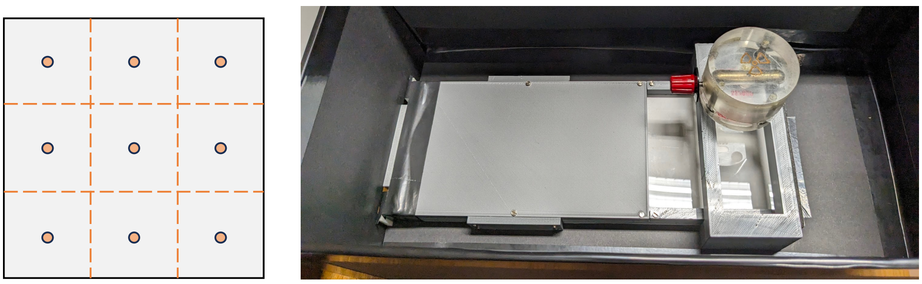

Figure 10: Set up of radiation measurement. Left figure shows how I divided the tile, and right figure shows how I put radiation source.

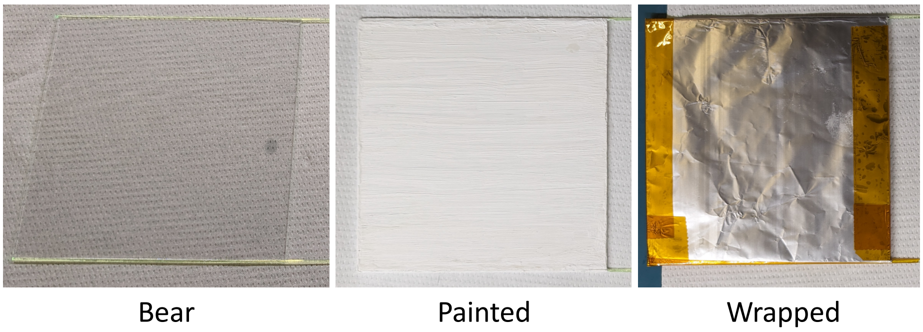

Figure 11: Three types of detector I used for radiation measurement. Left one is bear detector same as the one I used for dark pulse measurement. Middle one is detector with diffusive reflective paint of three layer. Right one is detector with aluminum foil of one layer. Foil was cut to fit the tile and wrapped the tile.

4.2 Analysis

Three values I mentioned were obtained from detected photon number distribution. This distribution was calculated by integrating Gaussian fit of photon peaks in integrated pulse distribution. The region of integral was defined as [Mean of Gaussian -3σ, Mean of Gaussian $+3\sigma$]. Then, detected photon number distribution was fitted by Landau function. Mean photon number was obtained from its fit parameters, and total detected photon number was calculated from the formula below.

$$\text{Total detected photon number} = \sum_{i=\text{First point}}^{\text{Last point}} (x \text{ of } i\text{th point}) \times (y \text{ of } i\text{th point}) \tag{2}$$

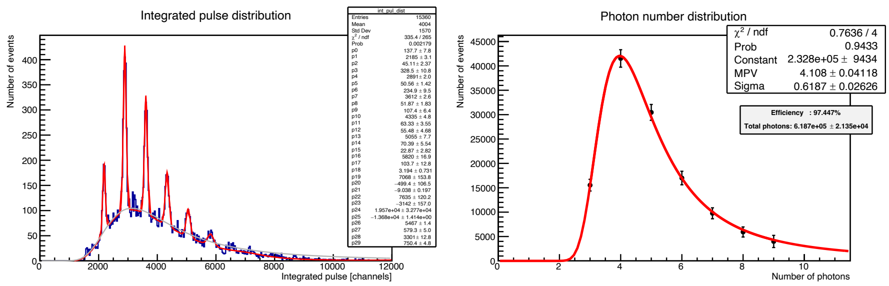

Figure 12: Example of integrated pulse distribution (left) and detected photon number distribution (right) of measurement with radiation source. In left figure, red line shows fitting curve of signal (multi-Gaussian) plus background (Landau), and gray line shows fitting curve of background. Number of events of peak is calculated from single-Gaussian whose parameters were obtained from red line. In right figure, red line shows fitting curve of Landau function.

Photon detection efficiency is confused because it should be calculated by the sum of signal from left and right SiPM but measurement of left and right SiPM was done independently in this study. Thus, I combined the signal from left and right SiPM as follows. First, I normalized the detected photon number distribution by dividing number of events of each point by the sum of them. Second, I multiply the normalized events of point of left SiPM and that of right SiPM for all pattern of combination. This value is the probability of getting the sum of detected photon number from left and right SiPM. Third, I plot the sum of detected photon number distribution and fit it by Landau function. Finally, photon detection efficiency was calculated from the formula below.

$$\text{Photon detection efficiency} = \frac{\int_{\text{Threshold}}^{\text{inf}} \text{Fitting curve}}{\int_{0}^{\text{inf}} \text{Fitting curve}} \tag{3}$$

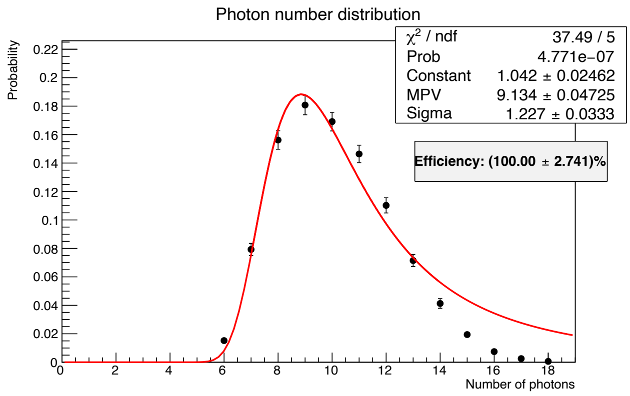

Figure 13: Example of the sum of detected photon number distribution. Red line shows fitting curve of Landau function.

4.3 Result

Fig14, 15 shows position dependence of detected photon number. Middle and bottom figure shows obvious position dependence both for left SiPM and right SiPM, but top figure shows that only for right SiPM. The increasing of obviousness in the middle and bottom figures compared to top is caused by the trapping of scintillation light, because paint and foil prevent photons to go outside the tile.

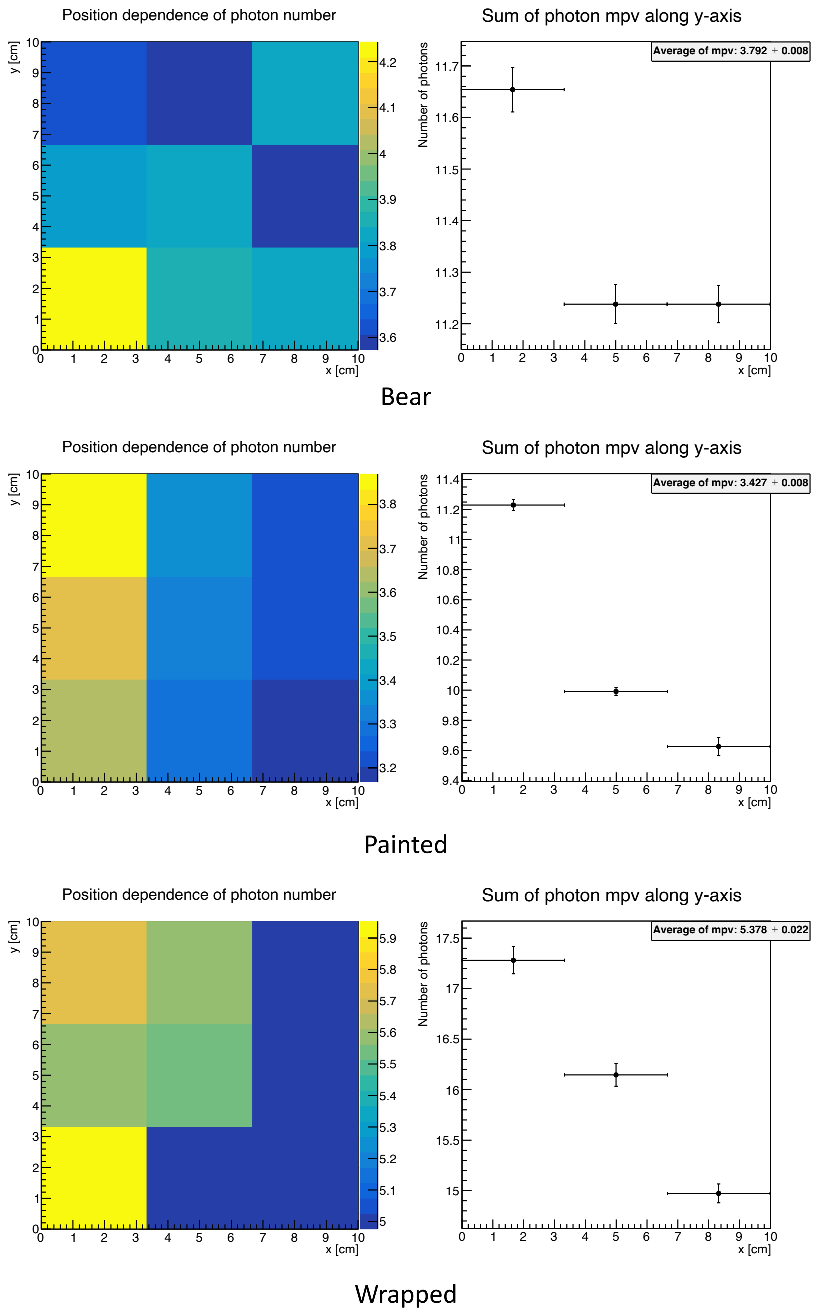

Figure 14: Position dependence of detected photon number in left SiPM. Top ones show the result of bear detector, middle ones show that of painted, and bottom ones show that of wrapped. In the left figure, wavelength shifting fiber is put along y-axis of $x = 0$, and SiPM is put on one end of the fiber of $y = 0$ side. Right figure shows the sum of mean detected photon number along y-axis.

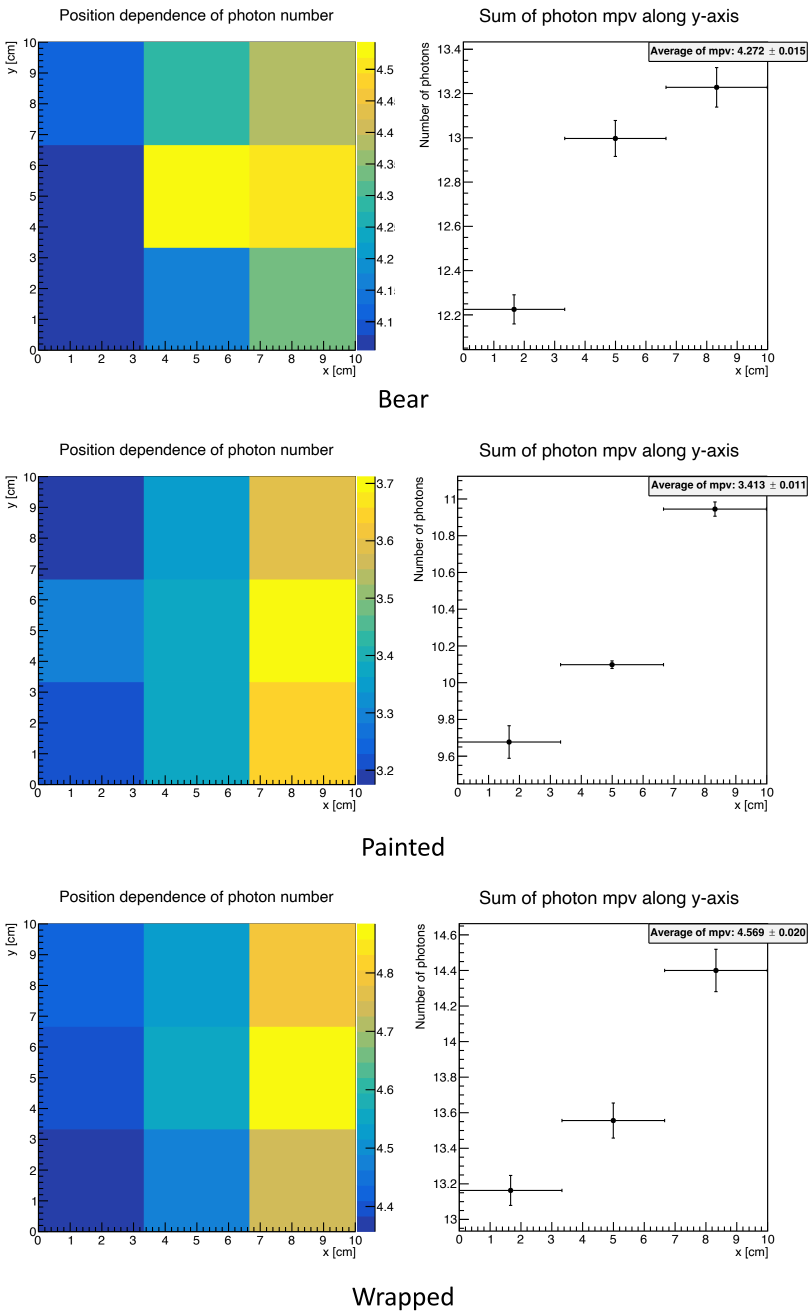

Figure 15: Position dependence of detected photon number in right SiPM. Top ones shows the result of bear detector, middle ones shows that of painted, and bottom ones shows that of wrapped. In the left figure, wavelength shifting fiber is put along y-axis of $x = 10$, and SiPM is put on one end of the fiber of $y = 0$ side. Right figure shows the sum of mean detected photon number along y-axis.

Table3 shows the mean detected photon number, total detected photon number, and photon detection efficiency for three types of detector. Values are the average of nine regions. It shows the decreasing of photon detection capability after painting and increasing of that after wrapping. This decreasing was caused by the trapping and absorption of light because diffusive reflective paint reflects light to random direction which does not let some fraction of light to go to fibers. On the other hand, foil reflects light to certain direction and guides it to the fibers smoothly. From this result, it is better to use reflective foil like aluminum foil to improve the capability of photon detection. Fig16 shows the position dependence of photon detection efficiency of wrapped detector. It does not shows the obvious position dependence of the efficiency. Although the efficiency is a bit lower than the goal of 99% in each position, it exceeds the goal on average, so it can conclude that threshold of three photons for each SiPM is good.

Table 3: Capability of photon detection for three different types of detector. Values are the average of nine regions, and Mean and Efficiency is combined result of left and right SiPM. Mean is mean detected photon number, Total is total detected photon number defined as Eq.(2), and Efficiency is photon detection efficiency defined as Eq.(3).

	SiPM	Mean	Total	Efficiency
Bear	left	8.824 ± 0.015	$(7.938 \pm 0.060) \times 10^5$	$(100.0 \pm 1.0)\%$
	right		$(6.296 \pm 0.071) \times 10^5$	
Painted	left	7.102 ± 0.011	$(6.120 \pm 0.045) \times 10^5$	$(100.0 \pm 1.0)\%$
	right		$(4.930 \pm 0.042) \times 10^5$	
Wrapped	left	10.867 ± 0.020	$(18.432 \pm 0.170) \times 10^5$	$(100.0 \pm 0.8)\%$
	right		$(8.733 \pm 0.012) \times 10^5$	

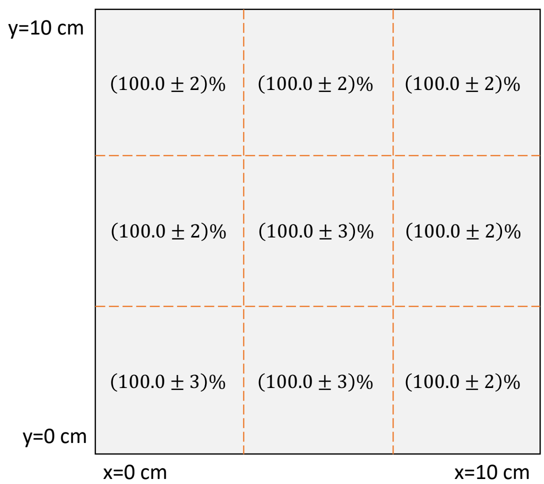

Figure 16: Position dependence of photon detection efficiency.

5 Conclusion

Test of scintillation tile detector with radiation source showed that it has dependence of detected photon number on the radiation injected position. Also, it showed that the threshold of three photons for each SiPM is good enough to achieve the goal of photon detection efficiency and less contamination of dark pulse. Comparison of three different types of detector showed that it is better to choose reflective foil like aluminum foil to improve the photon detection capability of detector and diffusive reflective paint has bad effect.

References

[1] Inaki Ortega Ruiz. Accurate profile measurement of the low intensity secondary beam in the CERN experimental areas. 2018.

[2] Robert Garbrecht Larsen. Development of radiation hard sensing fibres for FLASH therapy and the CERN Experimental Areas, Project report for CERN summer student programme 2022. 2022.